Electronic Supplementary Material (ESI) for Journal of Materials Chemistry C.

Supporting Information

Cu/Cu_2O nanocomposite as a p-type transparent-conductive-oxide for efficient bifacial-illuminated perovskite solar cells

You-Jyun Chen[a], Ming-Hsien Li[a], Jung-Chun-Andrew Huang[a,b,*], and Peter Chen[a,c,*]

[a]Department of Photonics, National Cheng Kung University, Tainan 701, Taiwan

[b]Department of Physics, National Cheng Kung University, Tainan 701, Taiwan

[c]Hierarchical Green-Energy Materials (Hi-GEM) Research Center, National Cheng Kung University, Tainan, 701, Taiwan

Corresponding authors.

E-mail addresses: jcahuang@mail.ncku.edu.tw (J.-C. Huang), petercyc@mail.ncku.edu.tw (P. Chen).

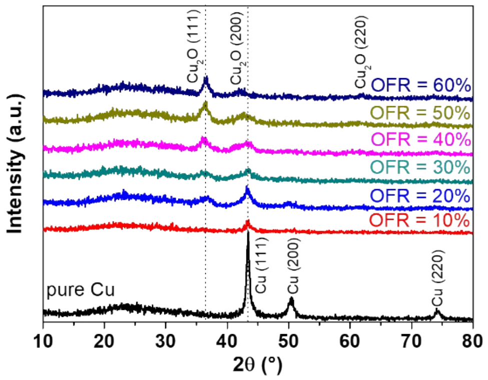

Figure S1. X-ray diffraction spectra of the Cu_2O films deposited at different OFRs from 10 to 60%. The pure Cu (OFR = 0%) film is also shown for comparison.[1]

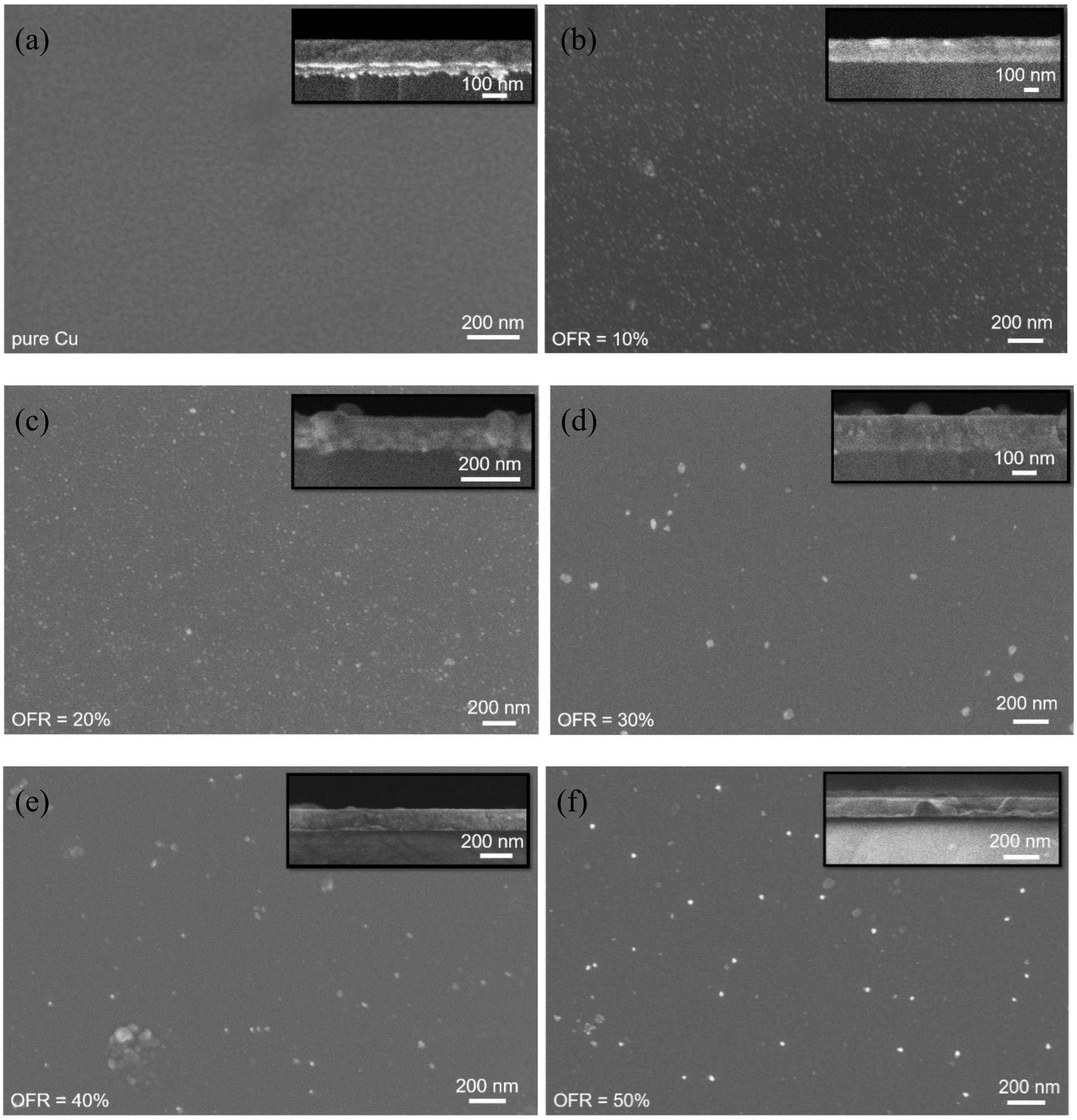

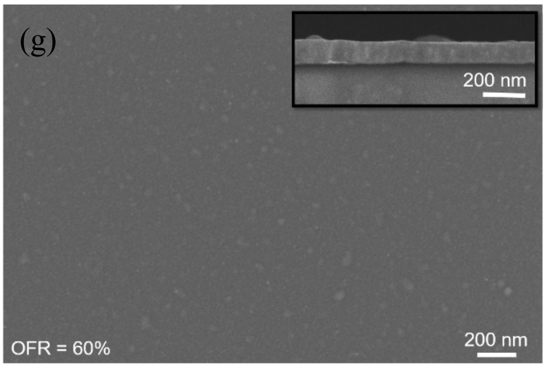

Figure S2. SEM images of the top-view of Cu/Cu_2O composite films with different oxygen flow ratios (a) 0%, (b) 10%, (c) 20%, (d) 30%, (e) 40%, (f) 50%, and (g) 60%. Insets show the corresponding cross-sectional SEM images.[1]

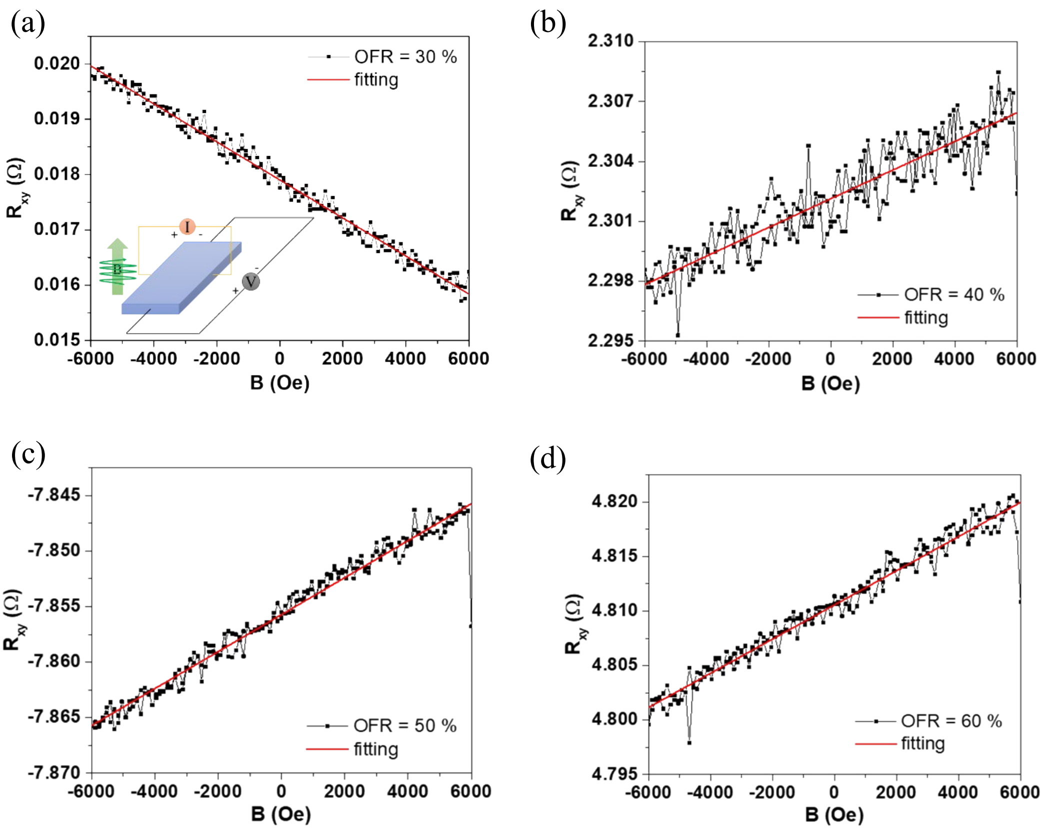

Figure S3. Hall effect measurements of the Cu/Cu_2O films with different oxygen flow ratios (a) 30%, (b) 40%, (c) 50%, and (d) 60%. Inset of (a) shows the input orientation of voltage, current, and magnetic field.[1]

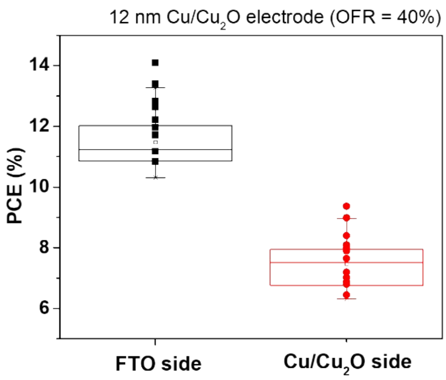

Figure S4. Statistical efficiency diagram of perovskite solar cells with Cu/Cu_2O electrodes (OFR = 40%) illuminated from FTO side and Cu/Cu_2O side, respectively.

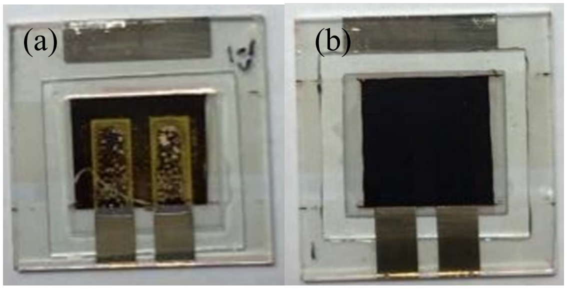

Figure S5. The photographs of the PSC using an (a) Ag as electrode and a (b) Cu/Cu_2O as electrode in dark surroundings for 55 days.

Table S1. The color change of growth films by bombarding copper target with 30 min with different argon and oxygen flow ratios.

color					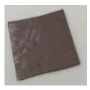	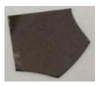	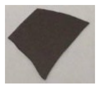
Ar(sccm)	5	4.5	4	3.5	3	3	3
O_2(sccm)	0	0.5	1	1.5	2	3	4.5
$\frac{O_2}{Ar+O_2}$	0%	10%	20%	30%	40%	50%	60%

Table S2. Electrical properties of Cu/Cu2O composite films under different oxygen flow ratios (OFRs).[1]

	Type	Thickness (nm)	Resistivity (Ω/square)	Resistance (Ω-cm)	Mobility (cm^2/V-s)	Concentration (cm^{-3})
OFR = 30%	n	20	78.82	1.58×10^{-4}	2.21	1.79×10^{22}
OFR =40%	p	20	72.5	1.45×10^{-4}	1.87	2.3×10^{22}
OFR = 50%	p	20	210.1	4.2×10^{-4}	1.23	8.54×10^{21}
OFR = 60%	p	20	83360	0.1667	60.5	6.19×10^{17}

Table S3. Comparison of performance of bifacial PSCs featuring various types of transparent electrodes.

Transparent electrode	Devcie architecture	Illumination side	PCE (%)	Reference
Carbon Nanotube	Glass/FTO/compact TiO_2/mesoporous TiO_2/ $CH_3NH_3PbI_3$/ Carbon Nanotube	FTO	6.87	[2]
	Glass/FTO/compact TiO_2/mesoporous TiO_2/$CH_3NH_3PbI_3$/Spiro-OMeTAD/Carbon Nanotube	FTO	9.9	
Au	Glass/FTO/compact TiO_2/ $CH_3NH_3PbI_{3-x}Cl_x$/Spiro-OMeTAD/Au	FTO	7.5	[3]
		Au	3	

Au	Glass/FTO/TiO_2/ $HC(NH_2)_2PbI_3$ /Spiro-OMeTAD/Au	FTO	5.2	[4]
Au/LiF	Glass/ITO/PEDOT:PSS/ $CH_3NH_3PbI_3$/ $PC_{60}BM$/Au/LiF	ITO	7.73	[5]
		Au/LiF	3.39	
MoO_3/Au/ MoO_3	Glass/FTO/TiO_2/$CH_3NH_3PbI_3$/Spiro-OMeTAD/ MoO_3/Au/MoO_3	FTO	13.0	[6]
		MoO_3/Au/MoO_3	9.7	
Graphene	Glass/FTO/compact TiO_2/$CH_3NH_3PbI_{3-X}Cl_X$/Spiro-OMeTAD/PEDOT:PSS+D-sorbitol/Graphene	FTO	12.02	[7]
		Graphene	11.65	
PEDOT	Glass/FTO/compact TiO_2/mesoporous TiO_2/$CH_3NH_3PbI_3$/PEDOT	FTO	12.33	[8]
		PEDOT	11.78	
PEIE/Ag/ MoO_x	Glass/ITO/PEDOT:PSS/$CH_3NH_3PbI_3$/PCBM/PEIE/Ag/MoO_x	ITO	13.55	[9]
		PEIE/Ag/ MoO_x	8.41	
BCP/Ag/ MoO_3	Glass/ITO/PEDOT:PSS/$CH_3NH_3PbI_3$/PCBM/C_{60}/BCP/Ag/ MoO_3	ITO	13.49	[10]
		BCP/Ag/MoO_3	9.61	
Cu/Cu_2O	Glass/FTO/compact TiO_2/mesoporous TiO_2/$CH_3NH_3PbI_3$/Spiro-OMeTAD/(Cu/Cu_2O)	FTO	14.1	This work
		Cu/Cu_2O	9.37	

Reference

1. Chen, Y.-J., et al., *Cu/Cu2O nanocomposite films as a p-type modified layer for efficient perovskite solar cells.* Scientific Reports, 2018 (accepted).
2. Li, Z., et al., *Laminated carbon nanotube networks for metal electrode-free efficient perovskite solar cells.* ACS nano, 2014. **8**(7): p. 6797-6804.
3. Eperon, G.E., et al., *Neutral color semitransparent microstructured perovskite solar cells.* ACS nano, 2013. **8**(1): p. 591-598.
4. Eperon, G.E., et al., *Efficient, semitransparent neutral-colored solar cells based on microstructured formamidinium lead trihalide perovskite.* The journal of physical chemistry letters, 2014. **6**(1): p. 129-138.
5. Roldán-Carmona, C., et al., *High efficiency single-junction semitransparent perovskite solar cells.* Energy & Environmental Science, 2014. **7**(9): p. 2968-2973.
6. Della Gaspera, E., et al., *Ultra-thin high efficiency semitransparent perovskite solar cells.* Nano Energy, 2015. **13**: p. 249-257.
7. You, P., et al., *Efficient semitransparent perovskite solar cells with graphene electrodes.* Advanced Materials, 2015. **27**(24): p. 3632-3638.
8. Xiao, Y., et al., *Efficient bifacial perovskite solar cell based on a highly transparent poly (3, 4-ethylenedioxythiophene) as the p-type hole-transporting material.* Journal of Power Sources, 2016. **306**: p. 171-177.
9. Pang, S., et al., *Efficient bifacial semitransparent perovskite solar cells with silver thin film electrode.* Solar Energy Materials and Solar Cells, 2017. **170**: p. 278-286.
10. Hanmandlu, C., et al., *Bifacial Perovskite Solar Cells Featuring Semitransparent Electrodes.* ACS applied materials & interfaces, 2017. **9**(38): p. 32635-32642.